Earth and Planetary Science Letters, 61 (1982) 211–219
Elsevier Scientific Publishing Company, Amsterdam – Printed in The Netherlands

[6]

Metal diagenesis in oxic marine sediments

G. Klinkhammer [1], D.T. Heggie [2] and D.W. Graham [2,*]

[1] *Earth Sciences Department, University of Leeds, Leeds, LS2 9JT (England)*
[2] *Graduate School of Oceanography, University of Rhode Island, Kingston, RI 02881 (U.S.A.)*

Received February 5, 1982
Revised version received August 13, 1982

The metal-nutrient relationships observed for nickel and cadmium in the deep ocean are continued at the interface between seawater and oxidizing pore water. This continuum results in pore water concentrations of these metals which are only slightly greater than near-bottom seawater levels. Manganese concentrations in these oxidizing pore waters are also extremely low, less than three times bottom water. In contrast, release in the boundary layer produces a maximum of dissolved copper which is 10–40 times ambient seawater.

Assuming these pore waters are at steady state, flux estimates based on these measurements suggest that the manganese in todorokite-rich nodules of the central equatorial Pacific was not supplied by upward diffusion through pore waters below the interface. Most nodular nickel is precipitated with manganese while nodular copper is supplied by diffusion.

1. Introduction

This paper presents concentration-depth profiles of manganese, copper, nickel and cadmium in oxidizing, abyssal pore waters. These data are important to our understanding of three fundamental processes associated with early diagenesis in deep-sea sediments.

Recycling of metals to seawater. With the advent of quality data we are beginning to identify trace elements which are vigorously recycled from deep-sea sediments. Water column profiles of copper [1], the rare earths [2] and beryllium [3] suggest a significant flux from sediments. It is clear that if we hope to understand the marine cycles of such elements we must learn a great deal more about early diagenesis in oxic sediments.

Diagenetic perturbations of the sedimentary record. The remobilization of certain elements during early diagenesis of suboxic sediments is so intense that it affects their distributions in the sediment column. Manganese is the best known example although copper and nickel also undergo redistribution during early suboxic diagenesis [4]. But suboxic sediments account for only a small fraction of the sea floor. This paper concerns the early diagenesis of metals in oxic sediments which are areally important but for which few reliable data are available.

Manganese nodule evolution. Since nodules grow at the sea-sediment interface the problems of nodule accretion and early diagenesis in sediments are closely associated. This study and its two companion papers [5,6] characterize the pore waters underlying an extensive nodule field. While the metal results do not offer any unequivocal answers concerning the evolution of these nodules they do constrain the problem considerably.

* Present address: Department of Chemistry, Woods Hole Oceanographic Institution, Woods Hole, MA 02543, U.S.A.

0012-821X/82/0000–0000/$02.75

2. Oceanographic settings

Pore water samples were collected at two sites in the central equatorial Pacific aboard R.V. "Knorr" during May 1979. Nutrient and carbonate chemistry results from these sites are presented elsewhere [5,6]. These locations were selected by the Manganese Nodule Program (MANOP) to represent typical provinces of siliceous (site S) and calcareous (site C) sedimentation.

Site S (11°02'N, 140°00'W) lies between the Clarion and Clipperton fracture zones and the water depth is 4910 m. The regional sedimentation rate is 2–3 mm/10^3 yr [7–9] but sedimentation at site S is variable. This region is renowned for its abundant copper- and nickel-rich manganese nodules [10]. Nodules are plentiful at site S and the specimens recovered here have todorokite mineralogy. The growth rates, chemistry and distribution of nodules at site S have been discussed by a number of authors [11–14].

The water depth at site C (01°03'N, 138°56'W) is 4430–4460 m. The sediment is virtually free of nodules and heavily bioturbated to 10 cm [15]. This site underlies the equatorial belt of productive surface waters which extends from the coast of South America to about 150°W [7]. The regional sedimentation rate at site C is at least 10 times faster than the average recent rate at site S. These differences in surface productivity and sedimentation are reflected in distinctly different pore water chemistries at these sites [5].

3. Methods

3.1. Sampling

Sediment samples with well preserved interfaces were collected as box cores and subsamples were taken with sections of plastic core liner within minutes of having come on board. These smaller cores were then extruded at 4°C and sliced into 2–3 cm intervals which were spun for 5 minutes at speeds up to 13,000 rpm with a Sorval Model SS-4 centrifuge. The supernatants were taken into a plastic syringe and forced through a 0.4-μm Nuclepore filter. Aliquots of these filtrates were acidified on board ship to pH 2 with redistilled HCl for subsequent trace metal analyses in the laboratory.

3.2. Analyses

Preconcentration. Cadmium, copper, nickel and iron were coprecipitated with ammonium pyrrolidine dithiocarbamate (APDC) and a cobalt carrier. Further details of these methods are given elsewhere [4]. The measurements reported here were made by atomic absorption spectrophotometry after preconcentrating 1- or 5-ml aliquots to 0.2 ml. Table 1 is a comparison between values for bottom water obtained using these small samples with those measured at the Massachusetts Institute of Technology using a similar technique but 40-ml aliquots [16] and measurements made by isotopic dilution at the University of Rhode Island [17]. Nickel was undetectable using 1-ml aliquots of bottom water; subsequently nickel in pore waters was measured after extracting 5 ml volumes. Manganese was extracted from acidified 5-ml aliquots using 8-hydroxyquinoline in chloroform [18]. In the worst case these bottom water manganese concentrations are two times the dissolved concentration [19] due to leaching of particulates after acidification of our samples.

Blanks and precisions. Subcores of three box cores from site S (62-2, 68-2, 101-8) and two cores from site C (21-2, 44-3) were separated for trace metal analyses. Blanks were estimated for each subcore by carrying seawater through our separation procedure. These blank experiments gave acceptable results for cadmium (0.02 nmol/kg), copper (0.6 nmol/kg) and nickel (0.6 nmol/kg). For some unknown reason the manganese blanks at site S were less satisfactory and only one core (101-8C) produced an acceptable value (0.05 nmol/kg). Consequently only manganese results for subcore 101-8C are reported for site S. With this exception the data summarized in Table 2 are mean concentrations $\pm$ one standard deviation for three cores from site S and two cores from site C. The analytical precision is better than $\pm$ 10%, which is less than the natural range at these sites. Unfor-

TABLE 1

Bottom water concentrations

	Technique	Metal (nmol/kg ± 1 std.dev.)			
		manganese	nickel	cadmium	copper
Site S					
Klinkhammer [4,18]	APDC/quinolinol	0.40	< 20	0.64 ± 0.07	6.0 ± 0.9
Mangum and Edmond [16]	APDC	–	8.0	0.65–0.70	5.0
Heggie [17]	isotope dilution	–	7.4 ± 0.2	0.64 ± 0.02	5.3
Site C					
Klinkhammer [4,18]	APDC/quinolinol	0.50	< 20	0.78 ± 0.05	7.0
Mangum and Edmond [16]	APDC	–	6.5	0.65–0.70	5.0

tunately, blank problems prevented us from detecting any systematic trends in dissolved iron. We can say that iron concentrations are less than 30 nmol/kg in the top 30 cm at both of these sites; this observation is consistent with the oxidizing character of these pore waters.

4. Results

Concentration-depth profiles at sites S and C (Fig. 1a, b) are distinctive. The most diagnostic metal at these sites is manganese. Sharply increasing dissolved manganese below 9 cm at site C is characteristic of suboxic pore waters [20] while site S sediments are clearly oxic (containing oxygenated pore waters) to 30 cm. Oxygen in the pore waters at site S [21] decreases with depth into the sediment but never falls below 40 μmol/kg in the top 30 cm. Interestingly, the data above 9 cm indicate that the diffusive flux of manganese is considerably larger at site C than at site S where nodules are abundant.

Nickel is released to pelagic pore fluids during the dissolution of manganese oxides [4]. This process is responsible for the prominent maximum of dissolved nickel in the suboxic zone at site C (Fig. 1b). Above 18 cm the nickel levels at site C are only two times greater than bottom water with the exception of the top interval. The manganese reduction zone was not encountered at site S and dissolved nickel is correspondingly low but never-

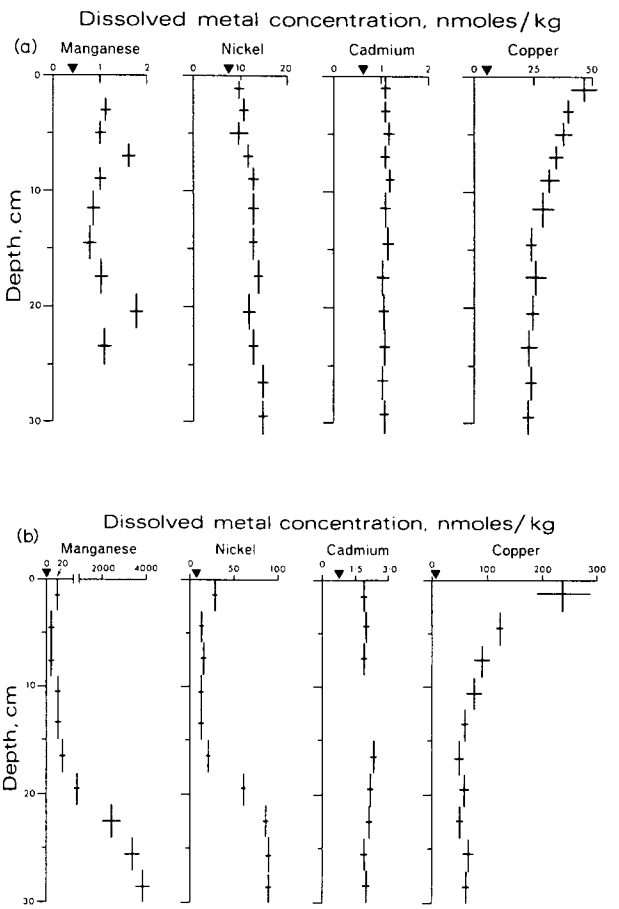

Fig. 1. Pore water profiles at MANOP site S (a) and MANOP site C (b). The arrow heads indicate bottom water concentrations.

theless slightly above bottom water. Thus, while the major feature of nickel diagenesis is release during suboxic reduction of manganese oxides, there is a small but significant increase across the interface of oxic sediments. While less spectacular than the remobilization during suboxic diagenesis this change is potentially more important to seawater chemistry and nodule evolution simply because it occurs near the boundary.

The cadmium concentration near the interface at site S is 1.8 times bottom water and remains constant or decreases slightly with depth. Dissolved cadmium in site C sediments is also fairly constant with depth but higher than at site S. Very little is known about cadmium geochemistry in deep-sea sediments but our calculations (section 5.2) suggest that these cadmium levels are reasonable.

Copper levels are highest in the top interval and decrease exponentially to essentially constant but different values at each site. Callender and Bowser [22] found similar dissolved copper concentrations at these locations. The profiles in Fig. 1 indicate a release of copper at the interface and removal at depth in the sediment. The core-top copper maximum at site S is 9 times greater than bottom water while at site C this feature is 40 times ambient seawater. In general, these copper profiles are similar to results from the Guatemala Basin and the East Pacific Rise [4]. This similarity is surprising considering the wide range of sedimentary environments sampled at these locations. Apparently diagenetic remobilization of copper is areally widespread but restricted to a thin layer at the interface (section 5.3).

5. Metal regeneration in oxic sediments

5.1. Introduction

One characteristic common to the metal profiles at the oxic site (S) (Fig. 1a) is that the steepest concentration gradient occurs across the sea-sediment interface. This observation implies that most metal regeneration in oxic sediments takes place near this boundary. Concentration-depth profiles are maintained by a coupling of this regeneration with varying degrees of interaction between dissolved metal and sediment below the interface. Manganese, nickel and cadmium show little tendency to react with the sediment under these conditions and their monotonic profiles at site S are generated by burial of surficial pore water. On the other hand copper is readily taken up by the sediment producing an exponential decrease with depth.

5.2. Nickel and cadmium regeneration

Degradation of residual organics that escape oxidation by the oxygenated water column is the driving force behind early sediment diagenesis. In pelagic regions (not underlying highly productive surface waters), e.g. site S, oxidation of organic matter in surface sediments is accomplished by consuming oxygen [23]. In the simplest case then, early diagenesis over much of the sea floor is analogous to oxidation in the overlying water column. The model developed in this section is based on this supposition, i.e. pore water near the interface is a continuum of ambient bottom water. If this hypothesis is correct it should be possible to predict the nickel and cadmium concentrations of surficial pore waters from interstitial nutrient concentrations since these metals are directly related to nutrients in seawater [24–26].

In this model we assume that metals and nutrients are lost from the interface by diffusion only so that the flux of metal M across the interface is related to the corresponding flux of nutrient N by a proportionately constant, M/N:

$$D_M \times \left.\frac{\mathrm{d}M}{\mathrm{d}z}\right|_{z=0} = \frac{M}{N} \times D_N \times \left.\frac{\mathrm{d}N}{\mathrm{d}z}\right|_{z=0} \qquad (1)$$

By assuming a linear concentration gradient across the interface, equation (1) reduces to the following relationship:

$$\frac{M}{N} = \frac{(M_0 - M_{BW}) \times D_M}{(N_0 - N_{BW}) \times D_N} \qquad (2)$$

Cadmium is related to the nitrate distribution in seawater [24,26] while nickel mimics silica in the deep ocean [25,26]. The appropriate diffusion coefficient ratios are: $D_{Cd}/D_{NO_3} = 0.36$, $D_{Ni}/D_{Si} = 0.68$ [27,28]. M_0 and M_{BW} are metal concentrations

TABLE 2

Pore water data for MANOP sites S and C

Depth (cm)	Nutrient (μmol/kg)		Metal (nmol/kg)			
	NO_3	Si	Mn	Ni	Cd	Cu
Site S						
Bottom water	36.1	144.1	0.40	7.7	0.64	5.4
0- 2	41.3	192.8	–	10	1.12 ± 0.11	47 ± 6
2- 4	43.0	230.9	1.10	11 ± 0	1.12 ± 0.18	40 ± 3
4- 6	44.1	258.1	1.00	10 ± 2	1.17 ± 0.08	38 ± 4
6- 8	44.8	273.7	1.69–1.55	12 ± 1	1.11 ± 0.06	35 ± 3
8–10	46.1	286.6	1.01	13	1.20 ± 0.10	32 ± 5
10–13	46.4	297.5	0.86	13 ± 1	1.15 ± 0.09	29 ± 5
13–16	47.5	307.5	0.86–0.73	13	1.16 ± 0.17	24 ± 2
16–19	47.5	311.7	1.01	14	1.06 ± 0.15	26 ± 4
19–22	48.4	314.5	1.68–1.89	12	1.07 ± 0.12	25 ± 2
22–25	48.4	319.9	1.11	13	1.09 ± 0.13	23 ± 4
25–28	48.5	326.0	–	15 ± 0	1.06 ± 0.15	24 ± 2
38–31	48.3	330.1	–	15 ± 2	1.07 ± 0.14	23 ± 2
Site C						
Bottom water	36.3	149.3	0.50	6.5	0.73	6.0
0- 3	45.5	305.9	19 ± 4	28 ± 8	1.90 ± 0.05	237 ± 49
3- 6	49.5	440.1	8.7 ± 4.3	14	2.00 ± 0.11	121 ± 8
6- 9	50.6	533.2	7.1	16 ± 0	1.95	93 ± 12
9–12	48.7	562.6	37 ± 2	13	–	76 ± 14
12–15	47.7	566.0	43 ± 3	13	–	62 ± 6
15–18	46.4	572.7	210 ± 150	20	2.37 ± 0.02	52 ± 10
18–21	45.2	576.0	880 ± 50	62 ± 2	2.27 ± 0.03	60 ± 13
21–24	44.4	572.7	2470 ± 450	87	2.20 ± 0.13	53 ± 7
24–27	43.9	576.9	3420 ± 400	90	1.89 ± 0.09	66 ± 6
27–30	42.4	576.9	3840 ± 290	90	1.96 ± 0.21	65 ± 13

in the top interval and bottom water (Table 2) while N_0 and N_{BW} are the corresponding nutrient levels.

A comparison of the results from equation (2) with the ratios observed in seawater (Table 3) is a test of continuity. The agreement for site S strongly supports the continuum model. The model is less satisfactory for the suboxic pore waters at site C, especially for nickel. This result is understandable since release of metals during the reduction of manganese oxides is a major consideration in such waters [4].

Since cadmium and nickel display nutrient-like behaviour across the seawater-pore water boundary

TABLE 3

Metal-nutrient ratios (M/N) calculated from equation (2) compared with those observed in seawater (SW) [24–26] and in the bottom waters (BW) at these sites (Table 2). For Ni, N = Si; for Cd, $N = NO_3$

	(M/N) $\times 10^5$	$(M/N)_{SW}$ $\times 10^5$	$(M/N)_{BW}$ $\times 10^5$
Site S			
Nickel	3.2	3.3	5.3
Cadmium	3.3	2.3	1.8
Site C			
Nickel	9.3	3.3	4.4
Cadmium	4.6	2.3	2.0

TABLE 4

The diffusive flux of metals from the oxidative sediments at MANOP site S compared with their accumulation rates in nodules and sediments in units of $\mu mol/cm^2\ 10^3$ yr. The first value listed for the diffusive flux of nickel and cadmium was calculated from equation (1) and the second from linear concentration gradients

	Diffusive flux	"Apple" nodule [11]		Average nodule [31]	Pelagic sediments [31]
		top	bottom		
Manganese	0.014	3.6	12.7	7.8	11
Nickel	0.040–0.094	0.13	0.73	0.26	0.43
Cadmium	0.015–0.021	–	–	–	–
Copper	1.8	0.059	0.42	0.14	0.53

their diffusive fluxes can be estimated from equation (1) and the appropriate nutrient fluxes. Fluxes from site S sediments predicted from advection-diffusion modeling [29] are 0.66 μmol NO_3/cm^2 yr and 1.2 μmol Si/cm^2 yr. Estimates of nickel and cadmium fluxes from linear concentration gradients agree well with those calculated from equation (1) (Table 4).

5.3. Copper regeneration

Clearly the model developed for nickel and cadmium is inappropriate for interstitial copper. The amount of copper released at the interface is much greater than would be predicted from decomposition of plankton for instance. We assume that these profiles are sustained by scavenging from the water column with vigorous recycling at the interface and removal in the sediment. This discussion is an effort to quantify these processes.

Removal in the sediment. The shapes of the dissolved copper profiles (Fig. 1) are in themselves diagnostic. The concentration gradients indicate diffusion upwards and downwards from the interface while the negative curvature is suggestive of uptake by sediment at depth. The simplest model consistent with our results is a steady-state approach where the copper profile is controlled by diffusion and first-order removal:

$$D\frac{\partial^2 C}{\partial z^2} - kC = 0 \qquad (3)$$

The solution of equation (3) for a one-layer sediment is given by the following expression [30]:

$$C = \frac{C_1 \sinh[R(h-z)] + C_2 \sinh(Rz)}{\sinh(Rh)} \qquad (4)$$

where $R = (k/D)^{1/2}$; C is the concentration predicted at depth z; C_1 and C_2 are the concentrations at the upper ($z = 0$) and lower ($z = h$) boundaries; D is the diffusion coefficient corrected for porosity, tortuosity and temperature [4] (1.4×10^{-6} cm^2/s) while k is the reaction rate constant in s^{-1}. Values for k were calculated by a best-fit approach. The data were modeled to about 15 cm since copper concentrations are statistically the same below this depth (Table 1 and Fig. 1). Having estimated k from the shapes of the profiles we can calculate the flux:

$$\text{downward flux} = \frac{DC_1R\cosh(Rh) - DRC_2}{\sinh(Rh)} \qquad (5)$$

The results of these calculations are summarized in Fig. 2 and Table 5.

The agreement displayed in Fig. 2 demonstrates that dissolved copper profiles in oxidizing pore waters are adequately explained by remobilization at the interface and removal below. The reaction rate constants for copper are much larger (by 10^4 to 10^6) than those obtained for silica, ammonia, calcium or magnesium in deep-sea sediments [30], emphasizing the vigorous nature of copper diagenesis. Moreover, our estimates of the amount of copper diffusing into these sediments (Table 5) bracket the average accumulation rate of copper in

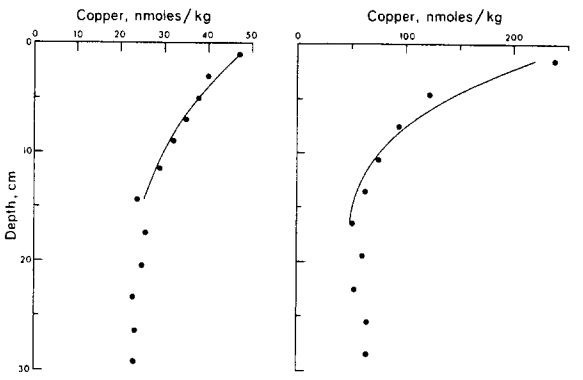

Fig. 2. Best-fit hyperbolic curves derived from equation (4) using the parameters in Table 5. The shaded circles are the measured concentrations for MANOP site S (the figure on the left) and site C.

pelagic sediments (Table 4) suggesting that most copper is diagenetic.

Recycling at the interface. Regeneration of copper produces a steep concentration gradient in the boundary layer which in turn drives a large diffusive flux into seawater. We can make a *conservative* estimate of this flux by assuming diffusion across a linear concentration gradient. The change across the interface at site S is $47 - 5.4 = 42$ nmol/kg over 1 cm. Multiplying this gradient by the corrected diffusion coefficient yields a flux of 1800 nmol/cm^2 10^3 yr from site S sediments. The corresponding estimate for site C is 6600 nmol/cm^2 10^3 yr. Recycling on this scale can maintain the entire copper inventory of the deep ocean [1,4].

Migration of copper to overlying seawater is at least ten times larger than diffusion into the sediment (Table 5) or the accumulation rate of copper in these sediments [22]. Since 90% of the copper escapes diffusion into the sediment, it must be released from a very thin layer at the surface. Also, since release of copper from *accumulating* sediment cannot maintain the surface maximum, this thin layer must be greatly enriched in copper compared with the bulk sediment. Assuming steady-state the copper content of this "enriched layer" is 2500–5000 ppm, i.e. the total copper content of the bulk sediment (500 ppm and 70 ppm at sites S and C, respectively [22]) multiplied by the ratio of the total diffusive flux to its accumulation rate (11 and 36 times, respectively). This calculation is only a rough approximation since the sedimentation rate at site S is extremely variable but it does demonstrate that there should be a pronounced surficial maximum in the solid copper content of these sediments.

Reactive copper must reside in a thin layer of fluff since analyses of 2-cm intervals from these sediments do not reveal a surficial anomaly [22]. Using this observation, limits on the thickness of the enriched layer, α, can be calculated from the mass balance for a two-layer, 2-cm slice of sediment:

$$\alpha = \frac{2[\mathrm{Cu}]_b - 2[\mathrm{Cu}]_s}{[\mathrm{Cu}]_f - [\mathrm{Cu}]_s} \tag{6}$$

Cu subscripts "s", "f" and "b" are the copper contents of the unenriched surface layer, the enriched film at the interface and the bulk sediment, respectively. $[\mathrm{Cu}]_b$ are measured concentrations and $[\mathrm{Cu}]_f$ was estimated previously. By definition we know that $0 \leqslant [\mathrm{Cu}]_s < [\mathrm{Cu}]_b$. Also, since $[\mathrm{Cu}]_s$

TABLE 5

Model parameters used in equations (4) and (5) to calculate the curves in Fig. 2 and the flux estimates below. These equations assume no production of copper from $z = 0$ (not the interface) to $z = h$

Site	C_1 (nmol/kg)	C_2 (nmol/kg)	h (cm)	k (yr^{-1})	Flux into the sediment (μmol/cm^2 10^3 yr)
S	47	26	13	0.17	0.11
C	220	50	15	0.86	1.3

$\ll [Cu]_f$ we can maximize α by setting $[Cu]_s = 0$. The resultant values of α are 0.2 cm at site S and 0.06 cm at site C. Apparently copper regeneration is truly a boundary layer process.

Our results indicate that copper is transported to the sea floor in a reactive coating. The scavenger may be organics which are consumed soon after deposition. In fact Soutar et al. [32] have presented evidence for a thin, carbon-rich layer covering pelagic sediments.

6. Diagenesis and nodule evolution at site S

This discussion is restricted to pore waters at MANOP site S and the todorokite-rich nodules that occur there. There is certainly an entire spectrum of pore water types and nodule chemistries to which our observations do not apply.

The diffusive flux of manganese to the interface at site S is at least 500 times less than its accumulation rate in nodules (Table 4). This result is intriguing since apparently manganese in the "apple" nodule recovered from site S was accumulating 3.5 times faster on the bottom than on the top [11]. Such contrast between nodule tops and bottoms is not peculiar to this particular nodule [33,34] and is often attributed to manganese reduction and diffusion through pore waters. Our results suggest that diffusion from below may not be responsible for this difference in site S nodules. Moreover, the rates of bioturbation in deep-sea sediments [35] are too slow to maintain this contrast.

Three mechanisms of nodule growth are consistent with these observations:

(1) *Non-steady-state*. Manganese accumulation in these nodules may respond to temporal changes in one or more sources. If indeed nodular manganese is influenced by diffusion through sediments or hydrothermal emanation, nodule growth must be episodic since neither pathway is important at the present time.

(2) *Diagenetic*. These nodules may grow by direct precipitation from unenriched bottom water and pore water. In this case one would expect similar concentration ratios: pore water/bottom water and nodule bottom/nodule top. These water-nodule ratios are 8.7–7.1 for copper, 1.3–5.6 for nickel and 2.8–3.5 for manganese (Tables 2, site S, and 4). This analysis suggests that nodular copper and manganese are influenced by diagenesis while there is another major source(s?) of nodular nickel.

(3) *Authigenic*. These nodules may grow partly by assimilation, oxidation and crystallization of amorphous manganese oxide grains produced in the water column. When these manganese oxides dissolve in the suboxic zone as at site C (Fig. 1b) they release a great deal of nickel (but little copper). The incorporation of these nickel-rich grains on nodule bottoms would explain the observed contrast.

7. Conclusions

There are distinct increases in the concentrations of dissolved manganese, nickel, cadmium and copper from bottom water to oxidizing pore water. The changes in nickel and cadmium across the sea-sediment interface are predictable from the nutrient concentrations of these pore waters and the metal-nutrient relationships observed in seawater. The corresponding change in copper is much larger. Regeneration of copper from a highly enriched veneer recycles copper to seawater nine times before eventual burial.

The manganese accumulation rates of todorokite nodules from the central equatorial Pacific are not sustained by steady-state molecular diffusion through pore waters. The diffusive flux can supply all the copper accumulating in these nodules but only part of the nickel.

Acknowledgements

Our thanks to R. Jahnke (Scripps Institution of Oceanography) and S. Emerson (University of Washington) for their help in collecting these samples. Harry Elderfield (University of Leeds) and Ed Boyd (Massachusetts Institute of Technology) proposed major changes which greatly improved the clarity of this manuscript. This work was supported by a grant to M. Bender (University of

Rhode Island) by the NSF, grant number OCE-77-05184 (MANOP).

References

1 E.A. Boyle, F.R. Sclater and J.M. Edmond, The distribution of dissolved copper in the Pacific, Earth Planet. Sci. Lett. 37 (1977) 38–54.

2 H. Elderfield and M.J. Greaves, The rare earth elements in seawater, Nature 296 (1982) 214–219.

3 C.I. Measures and J.M. Edmond, Beryllium in the water column of the central North Pacific, Nature 297 (1982) 52–53.

4 G. Klinkhammer, Early diagenesis in sediments from the eastern equatorial Pacific, II. Pore water metal results, Earth Planet. Sci. Lett. 49 (1980) 81–101.

5 R. Jahnke, D. Heggie, S. Emerson and V. Grundmanis, Pore waters of the central Pacific Ocean: nutrient results, Earth Planet. Sci. Lett. 61 (1982) 233–256 (this issue).

6 S. Emerson, V. Grundmanis and D. Graham, Carbonate chemistry in marine pore waters: MANOP sites C and S, Earth Planet. Sci. Lett. 61 (1982) 220–232 (this issue).

7 T.H. Van Andel, G.R. Heath and T.C. Moore Jr., Cenozoic History and Paleo-oceanography of the Central Equatorial Pacific Ocean, Geol. Soc. Am. Mem. 143 (1975).

8 D. Kadko, ^{230}Th, ^{226}Ra and ^{222}Rn in abyssal sediments, Earth Planet. Sci. Lett. 49 (1980) 360–380.

9 J.K. Cochran, The flux of ^{226}Ra from deep-sea sediment, Earth Planet. Sci. Lett. 49 (1980) 381–392.

10 J.L. Bischoff and D.Z. Piper, eds., Marine Geology and Oceanography of the Pacific Manganese Nodule Province (Plenum Press, New York, N.Y., 1979).

11 W. Moore, T-L. Ku, J. Macdougall, V. Burns, R. Burns, J. Dymond, M. Lyle and D. Piper, Fluxes of metals to a manganese nodule: radiochemical, chemical, structural and mineralogical studies, Earth Planet. Sci. Lett. 52 (1981) 151–171.

12 A. Huh, M. Kusakabe and T-L. Ku, Growth dynamics of manganese nodules at MANOP R and S sites—radioisotopic evidence, EOS 62 (1981) 905 (abstract).

13 M.D. Siegel and M. Fisk, Nodule chemistry, morphology and distribution in the abyssal hills surrounding MANOP site S, EOS 62 (1981) 905 (abstract).

14 W.S. Moore, M. Lyle and J. Dymond, Chemical and radiochemical differences in micro and macro nodules at MANOP site S, EOS 62 (1981) 905 (abstract).

15 M.W. Lyle and G.R. Heath, Carbonate sedimentation at MANOP site C, 1°N 139°W, equatorial Pacific, EOS 60 (1979) 850 (abstract).

16 B. Mangum and J.M. Edmond, EOS 60 (1979) 858 (abstract).

17 D. Heggie, A mass spectrometric technique for high precision analyses of Cu, Ni, An, Cd in sea waters, EOS 62 (1981) 906 (abstract).

18 G. Klinkhammer, Determination of manganese in sea water by flameless atomic absorption spectrometry after preconcentration with 8-hydroxyquinoline in chloroform, Anal. Chem. 52 (1980) 117–120.

19 W.M. Landing and K.W. Bruland, Manganese in the North Pacific, Earth Planet. Sci. Lett. 49 (1980) 45–56.

20 P.N. Froelich, G.P. Klinkhammer, M.L. Bender, N.A. Luedtke, G.R. Heath, D. Cullen and P. Dauphin, Early oxidation of organic matter in pelagic sediments of the eastern equatorial Atlantic: suboxic diagenesis, Geochim. Cosmochim. Acta 43 (1979) 1075–1090.

21 V. Grundmanis, personal communication.

22 E. Callender and C.J. Bowser, Manganese and copper geochemistry of interstitial fluids from nodule-rich pelagic sediments of the northeastern equatorial Pacific Ocean, Am. J. Sci. 280 (1980) 1063–1096.

23 V. Grundmanis and J.W. Murray, Aerobic respiration in pelagic marine sediments, Geochim. Cosmochim. Acta 46 (1982) 1101–1120.

24 E.A. Boyle, F. Sclater and J.M. Edmond, On the marine geochemistry of cadmium, Nature 263 (1976) 42–44.

25 F.R. Sclater, E. Boyle and J.M. Edmond, On the marine geochemistry of nickel, Earth Planet. Sci. Lett. 31 (1976) 119–128.

26 K.W. Bruland, Oceanographic distributions of cadmium, zinc, nickel and copper in the North Pacific, Earth Planet. Sci. Lett. 47 (1980) 176–198.

27 Y-H. Li and S. Gregory, Diffusion of ions in sea water and in deep-sea sediments, Geochim. Cosmochim. Acta 38 (1974) 703–714.

28 R. Wollast and R. Garrels, Diffusion coefficient of silica in seawater, Nature Phys. Sci. 229 (1971) 94.

29 F. Goloway, Diagenetic models of interstitial nitrate profiles in deep sea suboxic sediments, Msts. Thesis, University of Rhode Island (1980).

30 A. Lerman, Migrational processes and chemical reactions in interstitial waters, in: The Sea, 6, E.D. Goldberg, I.N. McCave, J.J. O'Brien and J.H. Steele, eds. (John Wiley and Sons, New York, N.Y., 1977) 695–738.

31 K. Boström, T. Kraemer and S. Gartner, Provenance and accumulation rates of opaline silica, Al, Ti, Fe, Mn, Cu, Ni and Co in Pacific pelagic sediments, Chem. Geol. 11 (1973) 123–148.

32 A. Soutar, S. Johnson, K. Fischer and J. Dymond, Sampling the sediment-water interface—evidence for an organic-rich surface layer, EOS 62 (1981) 905 (abstract).

33 W. Raab, Physical and chemical features of Pacific deep-sea manganese nodules and their implications to the genesis of nodules, in: Ferromanganese Deposits on the Ocean Floor, D.R. Horn, ed. (National Science Foundation, Washington, D.C., 1972) 31–49.

34 S.E. Calvert and N.B. Price, Geochemical variations in ferromanganese nodules and associated sediments from the Pacific Ocean, Mar. Chem. 5 (1977) 43–74.

35 D.R. Schink and N.L. Guinasso, Effects of bioturbation on sediment-seawater interaction, Mar. Geol. 23 (1977) 133–154.